Lithiophilite formation in granitic pegmatites: A reconnaissance experimental study of phosphate crystallization from hydrous aluminosilicate melts

JAMES E. SHIGLEY,* GORDON E. BROWN, JR.

Department of Geology, Stanford University, Stanford, California 94305

ABSTRACT

Crystallization of the pegmatite phosphate mineral lithiophilite, $Li(Mn^{2+},Fe^{2+})PO_4$, from hydrous aluminosilicate melts has been investigated experimentally to place some constraints on the conditions under which it can form from pegmatite melts. The starting materials for these reconnaissance experiments consisted of a mixture of minerals from the Li-rich Stewart pegmatite at Pala, California, plus varying amounts of water, chosen to model an inferred granite pegmatite melt composition. *P-T* conditions during the experiments were chosen to approximate those inferred for granite pegmatite formation at shallow depths (3–5 km). A Mn-Fe phosphate mineral, identified as lithiophilite on the basis of optical properties, microprobe data, and electron-diffraction patterns, was crystallized over a temperature range of 500–400°C (at 1.5 kbar) only from water-saturated melts (containing 3–11 wt% H_2O depending on temperature). Lithiophilite was accompanied by quartz but not by feldspar in these runs. Small amounts of sicklerite, $Li_{1-x}(Mn^{2+}_{1-x},Fe^{3+}_x)PO_4$, were also identified in some run products on the basis of optical properties.

These reconnaissance experiments suggest that coarse-grained lithiophilite crystallizes in the interior portions of complex granitic pegmatites as a primary phase from volatile-saturated magmas. No evidence was found for phosphate-silicate liquid immiscibility in the experimental run products, suggesting that such immiscibility is not necessary for lithiophilite formation in water-saturated granitic melts. The absence of feldspar in the run products is not consistent with the observed association of lithiophilite, quartz, and abundant K- and Na-feldspar in the upper intermediate microcline-quartz zone of the Stewart pegmatite. This discrepancy between natural and synthetic crystallization products may be due to (1) the complexing of Na, K, and/or Al by P in our simplified melt compositions, which should lower the activities of these elements and could suppress the crystallization of alkali feldspar; (2) the use of Pt capsule material in the experiments; and/or (3) the large amount of undercooling (300–400°C) in the crystallization runs. The presence of P in the melts appears to have had little effect on quartz crystallization, morphology, or growth rates relative to its crystallization in P-free melts of simpler composition. These experimental results support the hypothesis that lithiophilite, quartz, and alkali feldspar crystallized in the upper intermediate zone of the Stewart pegmatite from a water-saturated magma at temperatures of about 500°C or less and at pressures of about 1.5 kbar. The structural role of phosphorus in hydrous pegmatite melts is discussed and related to some of the experimental observations.

INTRODUCTION

Important among the accessory minerals in some granitic pegmatites are the phosphate species lithiophilite-triphylite $Li(Mn^{2+},Fe^{2+})PO_4$, which can occur as giant crystals up to several meters across and as smaller crystals or masses of intergrown crystals. Field observations indicate that these phosphates are primary phases which are commonly associated with alkali feldspar and quartz in the intermediate and core portions of internally zoned granitic pegmatites (Moore, 1973, 1982; Shigley and Brown, 1985). On the basis of their textural relationships and modes of occurrence, it is probable that these phosphates crystallized during the latter stages of granitic pegmatite formation. According to the genetic model of Jahns and Burnham (1969), crystallization of minerals during this period is facilitated by the presence of a coexisting, exsolved, volatile-rich fluid within the pegmatite magma system. Only a few experimental studies (e.g., Stewart,

1978; London, 1984, 1986) have attempted to relate accessory mineral paragenesis to the Jahns-Burnham model for crystallization of granitic pegmatites and to assess the roles of water and elements such as Li, F, Be, and B in the formation of accessory phases. No past experimental studies have provided information concerning the conditions under which primary phosphates crystallize in a pegmatite system.

The present experimental study was undertaken to gain a better understanding of the paragenesis of lithiophilite in pegmatites. It follows a recent field and analytical study of the well-known Stewart pegmatite in the Pala district, San Diego County, California (Shigley and Brown, 1985), which documented phosphate mineralogy and the alteration history of lithiophilite. This Li-rich pegmatite is one of the larger and more important of the numerous granitic pegmatites in the Pala area that are genetically related to the Mesozoic Peninsular Ranges (or Southern California) batholith (Larsen, 1948) and are thought to have crystallized at relatively shallow depths of several kilometers (Jahns and Wright, 1951; Taylor et al., 1979). Crystals of altered lithiophilite up to 40 cm in diameter occur in the microcline-quartz upper intermediate zone of the Stewart pegmatite.

The experimental conditions of this study were chosen to approximate the inferred P-T-X conditions of the Stewart pegmatite during its formation ($P = 1.5$ kbar; $T = 800$–$500°C$ or lower; Taylor et al., 1979). Our objectives were to place some constraints on the conditions under which lithiophilite crystallization could take place from a pegmatitic melt, to compare the phase assemblage from the experimental runs with the observed lithiophilite-bearing assemblage at the Stewart pegmatite, and to relate the experimental results to the paragenesis of primary phosphate minerals in this pegmatite. Because of the relatively small number of experimental runs and the lack of experimental reversals, this investigation should be viewed as a reconnaissance study.

EXPERIMENTAL METHODS

Starting materials consisted of a suite of natural minerals, most of which were collected at the Stewart pegmatite. Owing to a lack of suitable, unaltered Stewart lithiophilite, a sample of fresh lithiophilite from the Branchville, Connecticut, pegmatite (Stanford University collection #6072) was used for the phosphate component. The compositions of each of these phases are given in Table 1. The following mixture, used in each run, was selected to approximate the modal composition of the lithiophilite-bearing intermediate zone that forms a major portion of the pegmatite body (volume percents): quartz, 35%; microcline, 30%; albite, 15%; muscovite, 8%; lepidolite, 7%; and lithiophilite, 5%. These proportions also yield a bulk composition for the starting mixture that approximates Jahns' (1953) estimate of the bulk composition of the Stewart pegmatite (Table 1). Compared to most earlier studies of pegmatite crystallization, the starting mixture used here represents a more complex composition that should be closer to natural pegmatitic melts than one based on synthetic oxides; even so, it is missing minor modal constituents such as tourmaline and probably does not accurately reflect the minor elements or volatiles present during the formation of the Stewart pegmatite.

Optically homogeneous mineral fragments were selected, separately pulverized, and ground under acetone, resulting in grain sizes of 10–20 μm. Each sample was fired at 500–600°C in an open Pt crucible to remove any organic contaminants, and the powdered minerals were mixed in the desired proportions in an agate mortar and a McCrone Mill. Optical examination revealed the mixture to consist of irregular, broken fragments with an average diameter of less than 10 μm and a maximum diameter of less than 30 μm. To minimize the presence of Fe^{3+} and Mn^{3+}, the mixture was heated for 24 h at 600°C in a reducing atmosphere of forming gas (90% N_2 + 10% H_2). Following this treatment, no Fe^{3+} could be detected by wet chemical analysis. To prevent absorption of water, the mixture was kept in an evacuated dessicator until capsules were loaded.

Ten milligrams of this run mixture were loaded into 3-mm diameter Pt or AgPd capsules, each of which contained a known amount of freshly distilled and deionized water (1–11% of the total weight). These water contents were chosen to ensure that the aluminosilicate melts in different experimental runs spanned the range from water-undersaturated to water-saturated conditions. The capsules were sealed immediately after loading by arc welding and were placed in a vacuum oven for 12 h to test for leakage and to ensure an initially homogeneous water distribution. Capsule water contents are believed to be accurate to within 0.5 wt% of the quoted values.

Crystallization experiments were carried out in the Tuttle-Jahns Laboratory for Experimental Petrology at Stanford University using an internally heated pressure vessel modified after the design of Yoder (1950); the vessel was oriented in a horizontal position during the runs. An Inconel-sheathed Pt_{100}-$Pt_{90}Rh_{10}$ thermocouple, periodically calibrated against the melting points of Au (1064.4°C) and NaCl (801.2°C), was used for temperature measurement. Pressure was transmitted using Ar hydraulically pumped from a Harwood intensifier. Reported temperatures and pressures are believed to be accurate to ±10°C and ±100 bars, respectively. The 1.5-kbar pressure chosen for all runs corresponds to that for an estimated depth of formation of 3–5 km for the Stewart pegmatite (Jahns, 1953; Taylor et al., 1979). The fO_2 of the charge was not purposely constrained during each run and is unknown. The steel pressure vessel and Mo heater windings should result in an fO_2 below the FMQ buffer in the charge if it were in equilibrium with these components. This was probably not the case owing to the lower temperature of the pressure vessel and to the presence of water in the capsules, which could result in an increase in fO_2 if H_2 diffused out of the capsule. Therefore, the oxidation state of Fe in the charge is not known, although it is thought to be predominantly Fe^{2+} on the basis of past experience with Fe-bearing runs in these pressure vessels (P. M. Fenn, pers. comm., 1985). Small amounts (<20% of the total phosphate) of sicklerite, $Li_{1-x}(Mn^{2+}_{1-x},Fe^{3+}_x)PO_4$, were identified in some of the run products on the basis of optical properties, indicating that some Fe^{3+} was produced during the experiments.

Twelve successful experimental runs consisting of at least four capsules each were carried out and were typically several days to a week or more in duration. This relatively small number of successful runs and the lack of experimental reversals limit the accuracy of phase-assemblage boundaries. The liquidus temperature was found to be approximately 800°C for the compositions used in these experiments at 1.5 kbar. All of the runs involved an initial melting of the capsule contents at temperatures of 800°C or higher for periods ranging from 21 to 48 h (Table 2). Following initial melting and a heating interval during which a vapor phase exsolved from the melt (as indicated by bubbles in the glass and dimples on the glass surfaces), the run was rapidly cooled iso-

Table 1. Chemical compositions of starting materials and the run mixture

	Microcline	Albite	Muscovite	Lepidolite	Lithiophilite	Starting Mixture	Stewart pegmatite Jahns (1953)
SiO_2	64.3	67.7	46.2	64.8	0.52	74.7	74.9
Al_2O_3	19.3	20.4	36.4	18.3	0.1	12.1	14.9
Fe_2O_3	<0.04	0.06	1.12	<0.04	13.33	0.68	**
MnO	0.02	0.02	0.38	0.45	36.25	1.76	**
MgO	<0.10	<0.10	<0.10	<0.10	<0.10	<0.10	**
CaO	<0.02	<0.07	<0.02	<0.02	<0.07	<0.02	0.1
Na_2O	2.20	10.6	0.61	0.32	0.15	2.30	3.6
K_2O	13.0	0.38	9.86	7.32	0.03	4.89	5.2
Li_2O	0.05	0.06	0.37	3.29	8.78	0.66	0.7
TiO_2	<0.02	<0.02	<0.02	<0.02	<0.02	<0.02	**
P_2O_5	0.14	0.12	0.05	0.05	44.85	2.19	**
other	0.12	0.47	5.09	2.11	0.23	0.86	0.8
total	99.31	100.0	100.22	96.82	104.13	100.26	100.2

* All values in weight percent oxides. Analyses performed using X-ray and atomic absorption spectroscopy by J.S. Wahlberg, J. Taggart, J. Baker, and K. King of the USGS Analytical Branch, Lakewood, Colorado (Job #KS41).

** Not reported.

barically to a predetermined subliquidus temperature at which it was held for periods of 40–140 h to permit crystallization. The time required for this temperature drop varied with the amount of undercooling of the system but was on the order of several minutes. At the end of each run, final quenching at pressure was accomplished by turning off the furnace power; the pressure vessel reached room temperature within 20 min. Finally, the capsules were reweighed to check for possible volatile loss during the course of the run.

At the end of a run, the contents of each capsule were examined with a polarizing microscope. Powder X-ray diffraction data on run products were obtained using a Gandolfi camera and Ni-filtered, Cu $K\alpha$ radiation. Phases in several capsules were analyzed using an ARL-EMX-SM microprobe with wavelength-dispersive spectrometers. Well-analyzed natural spessartine, apatite, orthoclase, albite, and olivine were used as standards. An accelerating potential of 15 kV, an emission current of 0.02 μA, and a beam diameter of less than 10 μm were normal operating conditions. *ZAF* corrections were made using the program MAGIC IV (Colby, 1968). The relatively small size of the crystalline run products (1–30 μm) resulted in some uncertainty about microprobe compositions of the smaller grains. Therefore, as an aid

in phase identification, the crystalline phases in one capsule were examined using a Philips EM400 transmission electron microscope, which was equipped with an EDAX 711 energy-dispersive X-ray analyzer and operated at 100 kV.

RESULTS OF CRYSTALLIZATION EXPERIMENTS

Run conditions and results of the crystallization experiments are summarized in Table 2. Phase assemblages present in each of the successful runs are depicted in the pseudobinary temperature-composition diagram shown in Figure 1. Phase-assemblage field boundaries are believed to be accurate only to ±50°C and ±0.5 wt% H_2O and thus are shown as dashed lines.

Capsules from most of the crystallization runs contained a glass with vapor bubbles and one or more crystalline phases identified as quartz, lithiophilite, and minor sicklerite on the basis of optical properties, microprobe data, and electron-diffraction patterns. Figure 2 shows an optical photomicrograph of run 1–9 which contained dendritic groups of quartz crystals and vapor bubbles in glass.
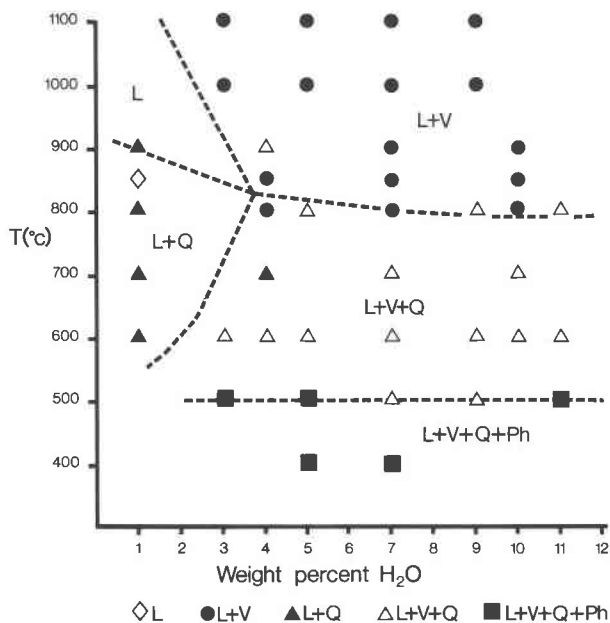
Fig. 1. Pseudobinary temperature-composition diagram showing the phase assemblages in the run products from 12 crystallization experiments. Boundaries separating phase-assemblage fields are marked by dashed lines and are believed to be accurate to ±50°C and ±0.5 wt% H_2O. The letters refer to the following phases: L = liquid (melt), V = vapor, Q = quartz, Ph = phosphate (primarily lithiophilite-triphylite).

An example of a run containing lithiophilite and quartz in glass (2–3) is shown in the back-scattered electron photomicrograph in Figure 3. These phases are described below in order of decreasing abundance.

Glass

The glass in each capsule is colorless to pale brown. A representative microprobe analysis of this glass (from capsule 1–9, which contains quartz but no other recognizable crystalline phase) gave (in weight percent) 74% SiO_2, 12% Al_2O_3, 5% K_2O, 2% Na_2O, 1% P_2O_5, 0.5% FeO, and 0.5% MnO; the remainder is presumably H_2O, Li_2O, and F. Some variations in glass composition were noted during microprobe analysis, with P_2O_5 ranging from 1 to 3.5 wt% (average = 2 wt%) for 46 spot analyses from glasses in 15 capsules that lacked phosphate crystals. These compositional inhomogeneities in some runs may indicate lack of equilibrium or they may have been caused, in part, by element diffusion during microprobe analysis. The glass is usually clear, but some areas exhibit cloudiness that is caused by numerous, small (<1 μm) objects that could be crystals, vapor bubbles, or globules of an immiscible liquid. Microprobe analyses of several of the cloudy areas showed them to have essentially the same composition as nearby clear or colored areas. TEM examination of one such cloudy area at high magnification (200,000×) failed to reveal any indication of liquid phase separation or small crystals. Past studies of phosphate-silicate liquid immis-
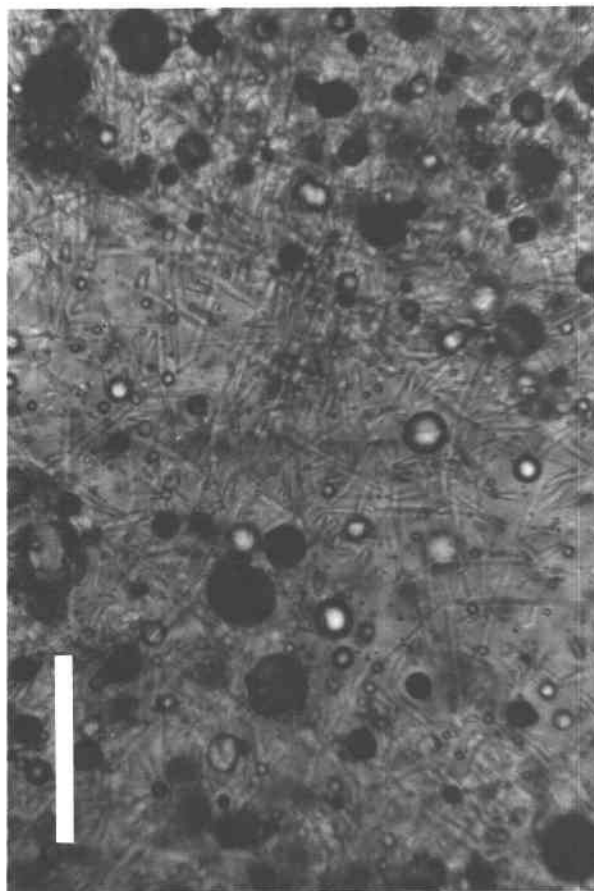

Fig. 2. Photomicrograph of dendritic groups of interlocking quartz crystals together with vapor bubbles in aluminosilicate glass from run capsule 1–9. Scale bar = 100 μm.

cibility using similar TEM techniques (James and McMillan, 1970) readily showed evidence for such immiscibility in quenched liquids from the Li_2O-SiO_2-P_2O_5 system. The TEM observations of the present study do not identify the cause of the cloudy areas but do tend to rule out silicate-phosphate liquid immiscibility.

All of the charges with greater than 1 wt% water contain numerous bubbles which vary in size, number, and distribution between charges (see Table 2 and Fig. 2). There is a significant increase in the number of vapor bubbles between charges with 3 and 5 wt% water, suggesting that the water-saturation level for melts of the run composition is near 4 wt% water. This value is similar to the saturation level of 4.6% water in granitic pegmatite melts at 1.5 kbar found by Burnham and Jahns (1958).

Quartz

Quartz is the most abundant crystalline phase present in the runs, occurring in all capsules that contained crystals and forming over a wide range of water contents (1–11 wt%) and temperatures (800°C and below). This phase was positively identified by electron diffraction and energy-dispersive X-ray analysis using the TEM; see Shigley

Table 2. Conditions and results of crystallization experiments

Run #	Initial Temp °C	Initial Pressure kbar	Duration hrs	Water Content %	Final Temp °C	Final Pressure kbar	Duration hrs	Est. Δ	Products	% of Crystals
1-1	800	1.5	52	1	600	1.3-1.2	120	400	L+Qz	75
1-3	800	1.5	52	3	600	1.3-1.2	120	300	L+V+Qz	15
1-5	800	1.5	52	5	600	1.3-1.2	120	200	L+V+Qz	<5
1-7	800	1.5	52	7	600	1.3-1.2	120	200	L+V+Qz	<5
1-9	800	1.5	52	9	600	1.3-1.2	120	200	L+V+Qz	10
1-11	800	1.5	52	11	600	1.3-1.2	120	200	L+V+Qz	5
2-1	800	1.5-1.4	47	1	-	-	-	-	*	-
2-3	800	1.5-1.4	47	3	500	1.2-1.1	117	400	L+V+Qz+Ph	<5
2-5	800	1.5-1.4	47	5	500	1.2-1.1	117	300	L+V+Qz+Ph	10
2-7	800	1.5-1.4	47	7	500	1.2-1.1	117	300	L+V+Qz	<5
2-9	800	1.5-1.4	47	9	500	1.2-1.1	117	300	L+V+Qz	20
2-11	800	1.5-1.4	47	11	500	1.2-1.1	117	300	L+V+Qz+Ph(?)	10
4-3	800	1.5-1.4	46	3	-	-	-	-	*	-
4-5	800	1.5-1.4	46	5	500	1.4	120	300	L+V+Qz+Ph	25
4-7	800	1.5-1.4	46	7	-	-	-	-	*	-
4-9	800	1.5-1.4	46	9	-	-	-	-	*	-
4-11	800	1.5-1.4	46	11	500	1.4	120	300	L+V+Qz+Ph	25
5-3	800	1.6	70	3	-	-	-	-	*	-
5-5	800	1.6	70	5	400	1.5	100	400	L+V+Qz+Ph	20
5-7	800	1.6	70	7	400	1.5	100	400	L+V+Qz+Ph	20
5-9	800	1.6	70	9	-	-	-	-	*	-
5-11	800	1.6	70	11	-	-	-	-	*	-
6-3	800	1.5	164	3	800	1.5	-	100	L+Qz	30
6-5	800	1.5	164	5	800	1.5	-	0	L+V+Qz	30
6-7	800	1.5	164	7	800	1.5	-	0	L+V+Qz	20
6-9	800	1.5	164	9	800	1.5	-	0	L+V+Qz	20
6-11	800	1.5	164	11	800	1.5	-	0	L+V+Qz	20
8-3	1000	1.5	48	3	1000	1.5	-	0	L+V	0
8-5	1000	1.5	48	5	1000	1.5	-	0	L+V	0
8-7	1000	1.5	48	7	1000	1.5	-	0	L+V	0
8-9	1000	1.5	48	9	1000	1.5	-	0	L+V	0
9-3	1100	1.6	21	3	1100	1.5	-	0	L+V	0
9-5	1100	1.6	21	5	1100	1.5	-	0	L+V	0
9-7	1100	1.6	21	7	1100	1.5	-	0	L+V	0
9-9	1100	1.6	21	9	1100	1.5	-	0	L+V	0
10-1	1100	1.6-1.5	28	1	900	1.5	95	100	L+Qz	15
10-4	1100	1.6-1.5	28	4	900	1.5	95	0	L+V+Qz	10
10-7	1100	1.6-1.5	28	7	900	1.5	95	0	L+V	0
10-10	1100	1.6-1.5	28	10	900	1.5	95	0	L+V	0
11-1	1100	1.4	28	1	850	1.4-1.2	95	150	L	0
11-4	1100	1.4	28	4	850	1.4-1.2	95	0	L+V	0
11-7	1100	1.4	28	7	850	1.4-1.2	95	0	L+V	0
11-10	1100	1.4	28	10	850	1.4-1.2	95	0	L+V	0
12-1	1100	1.5	30	1	800	1.4	42	200	L+Qz	20
12-4	1100	1.5	30	4	800	1.4	42	0	L+V	0
12-7	1100	1.5	30	7	800	1.4	42	0	L+V	0
12-10	1100	1.5	30	10	800	1.4	42	0	L+V	0
14-1	1100	1.7-1.5	47	1	700	1.5-1.4	137	300	L+Qz	80
14-4	1100	1.7-1.5	47	4	700	1.5-1.4	137	100	L+Qz	50
14-7	1100	1.7-1.5	47	7	700	1.5-1.4	137	100	L+V+Qz	20
14-10	1100	1.7-1.5	47	10	700	1.5-1.4	137	100	L+V+Qz	5
16-1	1100	2.0-1.9	24	1	600	1.7	141	400	L+Qz	10
16-4	1100	2.0-1.9	24	4	600	1.7	141	200	L+V+Qz	10
16-7	1100	2.0-1.9	24	7	600	1.7	141	200	L+V+Qz	10
16-10	1100	2.0-1.9	24	10	600	1.7	141	200	L+V+Qz	5

Column headings: Initial temp = homogenization temperature; Initial pressure = homogenization pressure; Final temp = temperature during crystallization; Final pressure = pressure during crystallization; Duration = time capsule held at temperature; est. Δ = estimated undercooling below liquidus; Products L = liquid (glass), V = vapor, Qz = quartz, Ph = phosphate mineral; % of crystals = total percentage of crystals in capsule at end of run. Pt capsules - runs # 1-7; AgPd capsules - runs # 8-16.

Column entries: runs # 6,8, and 9 held at higher temperature throughout experiment; * = capsule lost its volatile content and its constituents were unmelted at the end of the run.
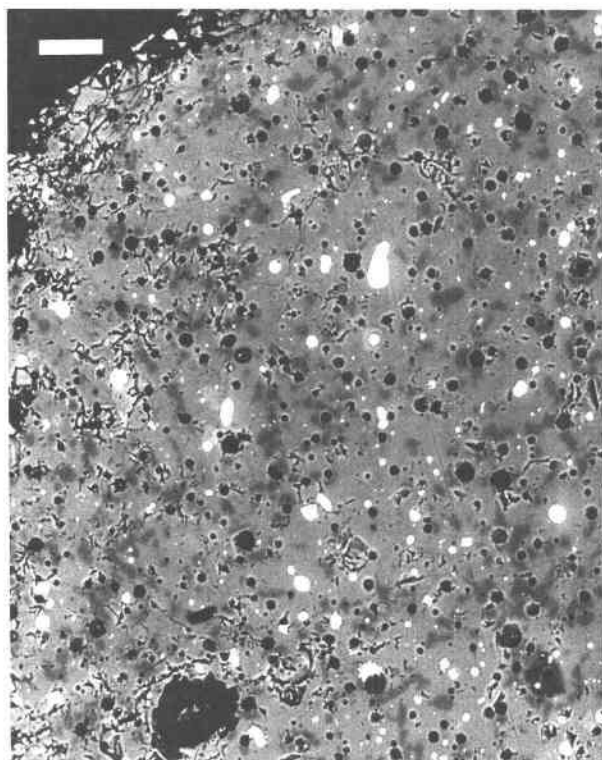
Fig. 3. Back-scattered electron photomicrograph of a polished thin section of aluminosilicate glass from run capsule 2–3. Grains of the Mn-Fe phosphate mineral identified as lithiophilite appear as white, spherical-, irregular-, or equant-shaped areas distributed throughout the glass. The dark-gray areas within the glass represent tabular quartz crystals. Scale bar = 50 μm.
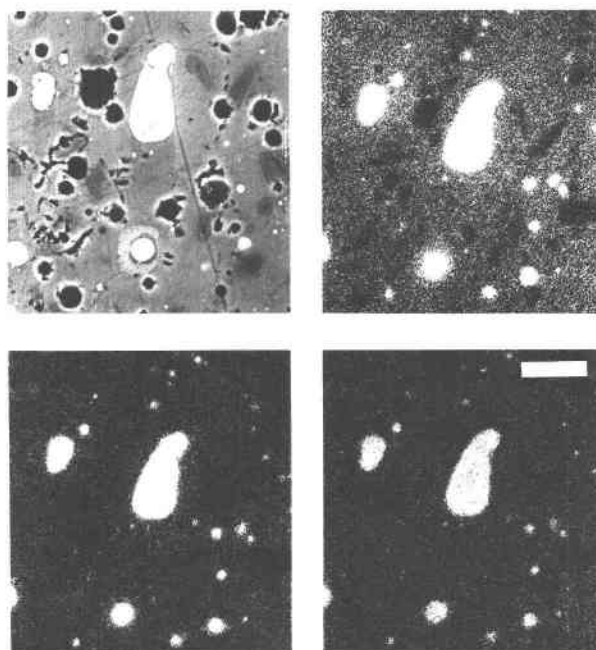

Fig. 4. Back-scattered electron photomicrograph (upper left) and corresponding $K\alpha$ X-ray maps for phosphorus (upper right), manganese (lower left), and iron (lower right) for lithiophilite grains in aluminosilicate glass from run capsule 2–3 (see Fig. 3). Scale bar, applicable to all four images, equals 25 μm. The white, irregular blebs are lithiophilite-triphylite crystals. The dark-gray objects within the glass shown in the back-scattered electron micrograph are quartz crystals, and the black features are holes formed by vapor bubbles. The sharp lines in this photomicrograph are scratches on the glass surface caused by polishing.

(1982) for details. The following types of quartz morphologies were observed: (1) tabular crystals of 5–25 μm in length and 5 μm in width; (2) acicular crystals of 25–75 μm in length and 5–10 μm in width; (3) dendritic groups of interlocking crystals up to several millimeters in size and showing uniform extinction; and (4) multicrystalline, spherulitic aggregates to several millimeters in size with radiating habit and wavy extinction.

These different quartz habits were not found together in the same capsule in most runs. The acicular and tabular crystals are more common in runs with higher water contents and smaller undercoolings, whereas the spherulitic crystals are more common in runs with higher water contents and larger undercoolings. A general decrease in the number of quartz crystals was observed with increasing water content. These observations are consistent with those from other crystallization studies of quartz and feldspar (Swanson et al., 1972; Fenn, 1973, 1977; Lofgren, 1974, 1980; Swanson, 1977; Fenn and Jahns, 1979; Swanson and Fenn, 1986). With the exception of some of the spherulites, most of the quartz crystals from the growth runs are suspended in the glass and are not attached to vapor bubbles or the capsule wall, suggesting that they nucleated internally. Minimum growth rates observed in these runs

ranged from 0.1×10^{-8} to 5×10^{-8} cm/s depending on crystal habit, with relative growth rates parallel to the **c** crystallographic axis being greater than those parallel to **a**. These rates are comparable to the growth rates for quartz (1.2 to 3.4×10^{-8} cm/s) crystallized from melts of Harding pegmatite and $Ab_{60}Q_{40}$ compositions (Swanson and Fenn, 1986).

Phosphates

Small (up to 30 μm), light- or reddish-brown grains of Mn-Fe phosphate were observed in runs 2, 4, and 5 (Table 2), which also contain quartz. These runs were at or above water saturation and were undercooled by 300–400°C. The grains generally appear as white, irregularly shaped blebs in back-scattered electron images (Fig. 3) and range in size from less than 5 μm to 30 μm. Some of the grains are tabular to euhedral crystals. Optical examination showed that most of these grains display moderate relief, moderate birefringence, uniform, straight extinction (noted for euhedral crystals), and little pleochroism. X-ray maps (Fig. 4) and microprobe analysis of these types of grains indicate the presence of Mn, Fe, and P in amounts consistent with the lithiophilite-triphylite solid-solution series (Table 3). Electron-diffraction patterns of one of

Table 3. Comparison of chemical data for lithiophilite

	phosphate grains in glass *	starting material **	stoichiometric composition ***
P_2O_5	45.52	44.85	45.22
$FeO^†$	5.31	11.99	0.0
MnO	37.72	36.25	45.22
Li_2O	n.d.[††]	8.78	9.56
other[†††]	0.62	1.03	0.0
total	89.17	102.90	100.00
total − Li_2O	89.17	94.12	90.44
(MnO+FeO)	43.03	48.24	45.22
(MnO/MnO+FeO)	0.87	0.75	1.00

```
*      average of five microprobe analyses of various phosphate grains in
       capsule 2-5
**     analysis of Branchville lithiophilite starting material with iron
       shown as FeO — see Table 1
***    ideal composition for LiMnPO₄
†      total iron reported as FeO
††     not determined
†††    SiO₂, Al₂O₃, K₂O, Na₂O
```

these grains gave *d*-spacings and relative intensities that are consistent with X-ray-diffraction data for lithiophilite (Blanchard, 1981); see Shigley (1982) for details. These observations indicate that most of the phosphate grains (>80%) produced in the experimental runs are members of the lithiophilite-triphylite solid-solution series. Microprobe traverses across the boundaries between lithiophilite and surrounding glass generally showed a sharp break with no evidence of an element depletion or enrichment halo around phosphate grains. Measured minimum growth rates for lithiophilite crystals, which are roughly equal in size to the tabular quartz crystals, are on the order of 1×10^{-8} cm/s.

A second type of phosphate grain, representing less than 20% of the total phosphate crystals present, is distinguishable from lithiophilite only on the basis of optical properties. These grains show high birefringence and reddish-brown pleochroism and are believed to be sicklerite.

Other phases

A small percentage (<5%) of the smaller, isolated, colorless crystals present in the run products clearly display inclined extinction and initially were thought to be alkali feldspars. Subsequent examination showed that none of these crystals exhibited a negative sign of elongation, which would be expected if they were alkali feldspars, based on

Fenn's (1973, 1977) observation that experimentally grown alkali feldspar crystals generally elongate along **a** rather than **c**. In addition, TEM examination of several of these crystals showed that they are not feldspar but did not lead to a unique identification.

DISCUSSION AND CONCLUSIONS

Lithiophilite paragenesis

The experimental results indicate that lithiophilite and minor sicklerite cocrystallized with quartz from a hydrous pegmatitic melt containing about 2 wt% P_2O_5 over the temperature interval 500°C to at least 400°C at about 1.5-kbar pressure. Water was above or near the saturation level (about 4 wt% H_2O) in all of the lithiophilite-producing runs; in the water-undersaturated runs (1 wt% H_2O) no lithiophilite was produced. These results suggest that crystallization of lithiophilite from a pegmatite melt is facilitated by the presence of an exsolved aqueous fluid phase; thus they are consistent with the presence of lithiophilite in the upper intermediate zone of the Stewart pegmatite which, according to the Jahns-Burnham model, is believed to have formed in the presence of an exsolved volatile fluid during the latter stages of pegmatite crystallization. These results are also consistent with the absence of lithiophilite from the lower, albite-rich inter-

mediate zone below the quartz core of the Stewart pegmatite, which is thought to have formed at the same time as the upper intermediate zone but not in the presence of an exsolved fluid phase (Jahns, 1982). The temperature interval reported above should be viewed as a minimum estimate for the formation of lithiophilite in the Stewart pegmatite; this is because of the failure of feldspar to nucleate and grow in the lithiophilite-producing runs may have caused a lowering of the temperature at which lithiophilite was saturated in the experimental melts.

Field examination of the phosphate-containing, upper quartz-microcline intermediate zone of the Stewart pegmatite (Shigley and Brown, 1985) showed that individual phosphate crystals or several intergrown crystals are separated from each other by 1 m or more. The larger the crystals or intergrowths were, the greater their separation from other phosphate crystals was. This scattered distribution suggests a relatively low density of lithiophilite nucleation sites in the pegmatite melt. The spacings among crystals suggest that even though the concentrations of Li, Mn, Fe, and P in the pegmatite melt at this stage of crystallization were sufficient to permit lithiophilite formation, these elements were dispersed over a relatively large volume around each growing crystal. As components were transported to the nucleation site, they were effectively depleted from this volume, which increased with the size of each crystal. Lithiophilite crystals in the experimental run products were scattered in a similar fashion (see Fig. 3), although their separations and sizes are much smaller. The hypothesis concerning element dispersion can be related to the inferred role of an exsolved fluid phase in lithiophilite growth from pegmatite melts. Although little is known about the partitioning behavior of Li, P, Mn, and Fe between silicate melt and a coexisting vapor phase, this water-rich phase could effect relatively rapid transport of these elements to the lithiophilite nucleation sites if they do partition into the vapor phase. In addition to this hypothesized mechanism, water dissolved in the melt would almost certainly lower viscosity and increase the diffusivity of these elements. Production of lithiophilite crystals only in experimental runs with water at or above the saturation level, however, favors the former mechanism. The element-dispersion hypothesis is also consistent with the lack of evidence for phosphate-silicate liquid immiscibility in the experimental runs without phosphate crystals, suggesting that such immiscibility is not necessary for lithiophilite formation in water-saturated pegmatite melts.

Absence of feldspar in run products

Considering the bulk composition of the run mixture, which is peraluminous and alkali-rich, the lack of feldspar crystals in the run products is surprising and inconsistent with the close association of lithiophilite, quartz, and alkali feldspar in the Stewart pegmatite. Both alkali and plagioclase feldspars have been crystallized from phosphate-free, natural and simplified, synthetic pegmatite melts over a similar range of P-T conditions and water contents (Fenn, 1973, 1977; Swanson et al., 1972; Lofgren, 1974; Fenn and Jahns, 1979; Fenn, 1986). Possible factors responsible for the absence of alkali feldspars in any of the crystallization runs from the present study include (1) the presence of phosphorus and its ability to form complexes with alkalis and aluminum; (2) the type of capsule material (Pt) used in most of these experiments; and (3) the large degree of undercooling employed for most of the crystallization runs. The discussion below suggests that the last two factors are more important than the first one in preventing the nucleation and growth of alkali feldspars.

Raman spectra of quenched, anhydrous, aluminosilicate melts with 1 to 5 mol% P_2O_5 (Mysen et al., 1981) have been interpreted as indicating the presence of M–PO_4 (M = Na,Ca) and AlPO_4 complexes in melts of different nonbridging oxygen to tetrahedral cation ratios (NBO/T). If such complexes, including K–PO_4, do form in P-containing pegmatite melts, the activities of Na, K, and Al should decrease, resulting in a reduction in the activities of feldspar components. The abundance of alkalis and aluminum, compared with the small amount of P_2O_5 in the melts of this experimental study, however, indicate that this proposed mechanism may not be the primary reason for the absence of alkali feldspars in the run products.

A more important reason for the absence of feldspars in the run products may involve the use of Pt capsule material for most of the crystallization runs. Fenn's unpublished work on feldspar growth from hydrous aluminosilicate melts (P. M. Fenn, 1985, pers. comm.) has shown that feldspars almost invariably nucleate on and grow from capsule walls; such growth is relatively easy on Au capsule walls, occurs to a limited extent on AgPd capsule walls, and is quite difficult on Pt capsule walls, especially for melts of pegmatite composition. These differences may be related to observed differences in H_2 diffusion rates through Au (low H_2 permeability), AgPd (intermediate H_2 permeability), and Pt (high H_2 permeability) and the resulting differences in catalytic activity of H_2 at capsule walls, or to differences in the catalytic activity of the different metals. If differences in H_2 permeability cause a greater build-up of H_2 near the Au capsule wall than near the Pt capsule wall, for example, there could be differences in depolymerization reactions of the aluminosilicate melt, involving H_2 or protons as catalysts, near the walls of different capsule materials. Recent work by Luth and Boettcher (1986) suggests that small amounts of H_2, from the dissociation reaction of H_2O, can dissolve in hydrous silicate melts, resulting in increases in solidus temperatures; however, little is known about the way in which H_2 interacts with the melt structure. If this interaction enhances melt depolymerization and the production of silicate monomers in the vicinity of Au capsule walls relative to Pt, the nucleation and growth of feldspars could be facilitated (cf. Taylor and Brown, 1979; deJong et al., 1981; Turnbull, 1985). Although highly speculative,

this mechanism could account for the relative differences in ease of feldspar nucleation on the walls of different capsule materials and for the lack of nucleation in the experiments reported here.

It is also likely that the large amount of undercooling in our phosphate- and quartz-producing runs (300–400°C) inhibited alkali feldspar nucleation. Fenn (1973) found that very small (25°C) or very large (465°C) undercoolings produced a significant kinetic or energetic barrier to the nucleation of feldspars from hydrous melts in the system Ab-Or-H$_2$O.

Structural role of P in aluminosilicate melts

Although typically a minor element in most aluminosilicate melts, phosphorus can have a dramatic influence on phase relations and other melt properties. In synthetic silicate melts, the presence of P$_2$O$_5$ has been shown to reduce liquidus temperatures (Tien and Hummel, 1962; Wyllie and Tuttle, 1964), to increase silicate tetrahedral polymerization and enlarge the liquidus stability fields of more polymerized silicate minerals (Kushiro, 1975), and to promote silicate liquid immiscibility and associated trace-element partitioning (Watson, 1976; Ryerson and Hess, 1978; Visser and Koster van Groos, 1979a, 1979b; Mysen et al., 1982). These effects should be magnified in the late-stage magmas, such as pegmatite melts, because of phosphorus enrichment in these melts as documented in field investigations (e.g., Murata and Richter, 1966; Henderson, 1968) and in experimental crystallization studies (e.g., Rutherford et al., 1974; Hess et al., 1975).

In silicate and phosphate melts and quenched melts, all available evidence suggests that phosphorus is tetrahedrally coordinated by oxygen (van Wazer, 1950; Westman and Crowther, 1954; Westman and Gartaganis, 1957; Meadowcraft and Richardson, 1965; Fraser, 1976; Ryerson and Hess, 1980; Mysen et al., 1981). In relatively depolymerized natural magmas and synthetic silicate melts (high NBO/T), where a variety of cations in addition to Si are present, the addition of P^{5+} is believed to cause formation of M–PO$_4$ orthophosphate complexes with nontetrahedral (M) cations such as Li, Na, K, Ca, Fe, Mn, which effectively removes them from their normal network-modifier roles (Ryerson and Hess, 1980; see also van Wazer and Callis, 1958). This assertion is based on a comparison of the enthalpies of formation of crystalline phosphates and silicates, which indicates that P–O–M bonds are energetically more stable than Si–O–M bonds. This preferential bonding of M cations with PO$_4$ tetrahedra in relatively depolymerized melts would produce an increase in Si–O–Si linkages and increase the tendency for silicate-phosphate liquid immiscibility (Hess, 1977). Mysen et al. (1981) suggested a different role for phosphorus in highly polymerized framework structure melts such as those of NaAlSi$_3$O$_8$ and CaAl$_2$Si$_2$O$_8$ compositions (NBO/T = 0; see Taylor and Brown, 1979); they interpreted Raman spectral data for quenched melts of these compositions as indicating that addition of phosphorus results in the formation of three-dimensional AlPO$_4$ com-

plexes as well as "sheetlike" P$_2$O$_5$ complexes. The suggested presence of AlPO$_4$ complexes implies that Na and Ca would be freed from their charge-balancing, network-forming role to become network modifiers, resulting in some depolymerization of the melt. In neither depolymerized nor fully polymerized aluminosilicate melts was Raman spectral evidence found for Si–O–P linkages (Mysen et al., 1981).

The above discussion is for anhydrous, P-bearing melts and does not apply directly to hydrous melts such as those from which pegmatites form. Water in such melts is thought to occur, in part, as OH$^-$ and, in part, as dissolved molecular H$_2$O below water-saturation levels (Stolper, 1982); above saturation levels, excess water exsolves from the melt to form a separate fluid phase. Raman spectral studies of chemically simple, hydrous, aluminosilicate melts with and without nonbridging oxygens (Mysen et al., 1982) were interpreted as indicating that water causes depolymerization. Thus the presence of phosphorus and water together in pegmatite melts should result in less depolymerization than with water and no phosphorus; this prediction assumes that pegmatite melts are not fully polymerized and that phosphorus does not form complexes with OH$^-$ or H$_2$O. This latter assumption may not be correct in light of the occurrence of P–OH bonds in numerous orthophosphate esters (see, e.g., Corbridge, 1971) and in some orthophosphate minerals such as hureaulite (Moore and Araki, 1973).

In the case of water-saturated pegmatite melts, such as those from which lithiophilite was grown in the present study, there is permissive evidence that phosphorus may partition into the exsolved aqueous-fluid phase. If this is, in fact, the case, some of the phosphorus would be removed from the melt and that fraction would no longer cause the structural changes suggested above.

This oversimplified and speculative picture of the "structure" of H$_2$O- and P-containing pegmatite melts can be used to help rationalize some of the experimental observations from the present study. The proposed formation of AlPO$_4$ and M–PO$_4$ complexes in pegmatite melts discussed earlier may account, in part, for the lack of feldspar nucleation and growth in the experimental runs. It was stated earlier that the addition of small amounts of phosphorus to a granite pegmatite melt has little effect on the growth rate of quartz. Because phosphorus is not predicted to form P–O–Si linkages and may partition into the exsolved aqueous-fluid phase, it should have little effect on the mobility of SiO$_4$ tetrahedra or on the growth rate of quartz in water-saturated melts.

The phosphates produced in the present experimental work and occurring in the Stewart pegmatite and in other natural phosphate parageneses are orthophosphates, i.e., their structures are made up of isolated PO$_4$ tetrahedra which are linked by nontetrahedral cations. Byrappa (1983) has shown in hydrothermal synthesis experiments that condensed phosphates are not stable in the presence of water. In contrast, synthesis of phosphates from anhydrous melts results in pryo-, ring-, chain-, and sheet-phos-

phate structures (Corbridge, 1971). Thus water must depolymerize phosphate structural units such as the proposed "sheetlike" P_2O_5 units (Mysen et al., 1981) and other proposed polymerized units (see Fraser, 1976) in hydrous silicate melts, resulting in the formation of orthophosphates; this depolymerization in H_2O-containing silicate melts also should promote the dispersal of PO_4 tetrahedra and reduce the probability of phosphate-silicate liquid immiscibility. No evidence was found for such immiscibility in quenched melts from the present study.

Additional experimental and spectroscopic work, especially on the partitioning behavior of phosphorus between melt and exsolved aqueous-fluid phase, is needed to verify some of the ideas presented above and to further elucidate the structural role of phosphorus in hydrous aluminosilicate melts, including those that contain boron. The recent experimental study by London (1986) suggests that boron and lithium are fractionated into residual pegmatitic fluids. This fractionation causes an increase in the silicate melt–H_2O miscibility to a point where there could be extensive rehomogenization of silicate melt and an exsolved aqueous-fluid phase during the latter stages of pegmatite crystallization. Thus certain aspects of the Jahns-Burnham model that pertain to the role of an exsolved volatile fluid during pegmatite crystallization may need re-evaluation. Additional experimental data for P-bearing, hydrous silicate melt systems also are needed before predictions of equilibrium properties of melts like those made by Burnham and Nekvasil (1986) will be possible for P-containing pegmatite melts.

REFERENCES

Blanchard, N. (1981) X-ray powder diffraction data for lithiophilite. Florida Scientist, 44, 53–56.

Burnham, C. Wayne, and Jahns, R.H. (1958) Experimental studies of pegmatite genesis: The solubility of water in granitic magmas. [abs.] Geological Society of America Bulletin, 69, 1544–1545.

Burnham, C. Wayne, and Nekvasil, Hanna. (1986) Equilibrium properties of granite pegmatite magmas, 71, 239–263.

Byrappa, K. (1983) The possible reasons for the absence of condensed phosphates in nature. Physics and Chemistry of Minerals, 10, 94–95.

Colby, J.W. (1968) Quantitative analysis of thin insulating films. Advances in X-ray Analysis, 11, 287–303.

Corbridge, D.E.C. (1971) The structural chemistry of phosphates. Bulletin de la Société française de Minéralogie et de Cristallographie, 94, 271–299.

deJong, B.H.W.S., Keefer, K.D., Brown, G.E., Jr., and Taylor, C.M. (1981) Polymerization of silicate and aluminate tetrahedra in glasses, melts, and aqueous solutions—III. Local silicon environments and internal nucleation in silicate glasses. Geochimica et Cosmochimica Acta, 45, 1291–1308.

Fenn, P.M. (1973) Nucleation and growth of alkali feldspars from melts in the system $NaAlSi_3O_8$–$KAlSi_3O_8$–H_2O. Ph.D. thesis, Stanford University, Stanford, California.

——— (1977) The nucleation and growth of alkali feldspars from hydrous melts. Canadian Mineralogist, 15, 135–161.

——— (1986) On the origin of graphic granite. American Mineralogist, 71, 325–330.

Fenn, P.M., and Jahns, R.H. (1979) Experimental crystallization of Harding, New Mexico, pegmatite. Geological Society of America, Abstracts with Programs, 11, 77–78.

Fraser, D.G. (1976) Thermodynamic properties of silicate metls. In D.G. Fraser, Ed. Thermodynamics in geology, 301–325. D. Reidel Publishing Company, Dordrecht-Holland.

Henderson, P. (1968) The distribution of phosphorus in the early and middle stages of fractionation of some basic layered intrusions. Geochimica et Cosmochimica Acta, 32, 897–911.

Hess, P.C. (1977) Structure of silicate melts. Canadian Mineralogist, 15, 162–178.

Hess, P.C., Rutherford, M.J., Guillemette, R.N., Ryerson, F.J., and Tuchfeld, H.A. (1975) Residual products of fractional crystallization of lunar magmas: An experimental study. Proceedings of the 6th Lunar Science Conference, 1, 895–909.

Jahns, R.H. (1953) The genesis of pegmatites: II. Quantitative analysis of lithium-bearing pegmatite, Mora County, New Mexico. American Mineralogist, 38, 1078–1112.

——— (1982) Internal evolution of granitic pegmatites. In P. Černý, Ed. Granitic pegmatites in science and industry, 293–327, Mineralogical Association of Canada Short Course Handbook 8.

Jahns, R.H., and Burnham, C.W. (1969) Experimental studies of pegmatite genesis: I. A model for the derivation and crystallization of granitic pegmatites. Economic Geology, 64, 863–864.

Jahns, R.H., and Wright, L.A. (1951) Gem- and lithium-bearing pegmatites of the Pala district, San Diego County, California. California Division of Mines Special Report, 7A, 1–70.

James, P.F., and McMillan, P.W. (1970) Quantitative measurements of phase separation in glasses using transmission electron microscopy. Part 2. A study of lithia-silica glasses and the influence of phosphorus pentoxide. Physics and Chemistry of Glasses, 11, 64–70.

Kushiro, Ikuo. (1975) On the nature of silicate melt and its significance in magma genesis: Regularities in the shift of the liquidus boundaries involving olivine, pyroxenes, and silica minerals. American Journal of Science, 275, 411–431.

Larsen, E.S. (1948) Batholith and associated rocks of Corona, Elsinore and San Luis Rey quadrangles, Southern California. Geological Society of America Memoir 29.

Lofgren, G.E. (1974) An experimental study of plagioclase crystal morphology: Isothermal crystallization. American Journal of Science, 274, 243–273.

——— (1980) Experimental studies of dynamic crystallization of silicate melts. In R.B. Hargraves, Ed. Physics of magmatic processes, 487–551. Princeton University Press, Princeton, New Jersey.

London, David. (1984) Experimental phase equilibria in the system $LiAlSiO_4$-SiO_2-H_2O: A petrogenetic grid for lithium-rich pegmatites. American Mineralogist, 69, 995–1004.

——— (1986) The magmatic-hydrothermal transition in the Tanco rare-element pegmatite: Evidence from fluid inclusions and phase-equilibria experiments. American Mineralogist, 71, 376–395.

Luth, R.W., and Boettcher, A.L. (1986) Hydrogen and the melting of silicates. American Mineralogist, 71, 264–276.

Meadowcraft, T.R., and Richardson, F.D. (1965) Structural and thermodynamic aspects of phosphate glasses. Faraday Society Transactions, 61, 54–70.

Moore, P.B. (1973) Pegmatitic phosphates: Descriptive mineralogy and crystal chemistry. Mineralogical Record, 4, 103–130.

——— (1982) Pegmatite minerals of P (V) and B (III). In P. Černý, Ed. Granitic pegmatites in science and industry, 267–291, Mineralogical Association of Canada Handbook 8.

Moore, P.B., and Araki, Takahura. (1973) Hureaulite, $Mn_5^{2+}(H_2O)_4[PO_3(OH)]_2[PO_4]_2$: Its atomic arrangement. American Mineralogist, 58, 302–307.

Murata, K.J., and Richter, D.H. (1966) Chemistry of the lavas of the 1959–60 eruption of Kilauea volcano, Hawaii. U.S. Geological Survey Professional Paper, 537A, 1–26.

Mysen, B.O., Ryerson, F.J., and Virgo, David. (1981) The structural role of phosphorus in silicate melts. American Mineralogist, 66, 106–117.

Mysen, B.O., Virgo, David, and Seifert, F.A. (1982) The structure of silicate melts: Implications for chemical and physical properties of natural magmas. Reviews of Geophysics and Space Physics, 20, 353–383.

Rutherford, M.J., Hess, P.C., and Daniel, G.H. (1974) Experimental liquid line of descent and liquid immiscibility for basalt 70017. Proceedings of the 5th Lunar Science Conference, 1, 569–583.

Ryerson, F.J., and Hess, P.C. (1978) Implications of liquid-liquid distribution coefficients to mineral-liquid partitioning. Geochimica et Cosmochimica Acta, 42, 921–932.

——— (1980) The role of P_2O_5 in silicate melts. Geochimica et Cosmochimica Acta, 44, 611–624.

Shigley, J.E. (1982) Phosphate minerals in granitic pegmatites: A study of primary and secondary phosphates from the Stewart pegmatite, Pala, California. Ph.D. thesis, Stanford University, Stanford, California.

Shigley, J.E., and Brown, G.E., Jr. (1985) Occurrence and alteration of phosphate minerals at the Stewart pegmatite, Pala district, San Diego County, California. American Mineralogist, 70, 395–408.

Stewart, D.B. (1978) Petrogenesis of lithium-rich pegmatites. American Mineralogist, 63, 970–980.

Stolper, Edward. (1982) The speciation of water in silicate melts. Geochimica et Cosmochimica Acta, 46, 2609–2620.

Swanson, S.E. (1977) Relation of nucleation and crystal-growth rate to the development of granitic textures. American Mineralogist, 62, 966–978.

Swanson, S.E., and Fenn, P.M. (1986) Quartz crystallization in igneous rocks. American Mineralogist, 71, 331–342.

Swanson, S.E., Whitney, J.A., and Luth, W.C. (1972) Growth of large quartz and feldspar crystals from synthetic granitic liquids. (abs.) EOS (American Geophysical Union Transactions), 53, 1127.

Taylor, B.E., Foord, E.E., and Friedrichsen, H. (1979) Stable isotope and fluid inclusion studies of gem-bearing granitic pegmatite-aplite dikes in San Diego County, California. Contributions to Mineralogy and Petrology, 68, 187–205.

Taylor, M.P., and Brown, G.E., Jr. (1979) The structure of mineral glasses: I. The feldspar glasses $NaAlSi_3O_8$, $KAlSi_3O_8$, $CaAl_2Si_2O_8$. Geochimica et Cosmochimica Acta, 43, 61–77.

Tien, T.Y., and Hummel, F.A. (1962) The system SiO_2-P_2O_5. American Ceramic Society Journal, 45, 422–424.

Turnbull, David. (1985) Dependence of crystallization rate on amorphous structure. Journal of Non-Crystalline Solids, 75, 197–208.

van Wazer, J.R. (1950) Structure and properties of condensed phosphates: II. A theory of molecular structure of sodium phosphate glasses. American Chemical Society Journal, 72, 644–647.

van Wazer, J.R., and Callis, C.F. (1958) Metal complexing by phosphates. Chemical Review, 58, 1011–1043.

Visser, W., and Koster van Groos, A.F. (1979a) Effects of P_2O_5 and TiO_2 on liquid-liquid equilibria in the system K_2O-FeO-Al_2O_3-SiO_2. American Journal of Science, 279, 970–988.

——— (1979b) Effect of pressure on liquid immiscibility in the system K_2O-FeO-Al_2O_3-SiO_2-P_2O_5. American Journal of Science, 279, 1160–1175.

Watson, E.B. (1976) Two-liquid partition coefficients: Experimental data and geochemical implications. Contributions to Mineralogy and Petrology, 56, 119–134.

Westman, A.E.R., and Crowther, J. (1954) Constitution of soluble phosphate glasses. American Ceramic Society Journal, 37, 420–426.

Westman, A.E.R., and Gartaganis, P.A. (1957) Constitution of sodium, potassium, and lithium phosphate glasses. American Ceramic Society Journal, 40, 293–298.

Wyllie, P.J., and Tuttle, O.F. (1964) Experimental studies of silicate systems containing two volatile components: II. The effects of SO_3, P_2O_5, HCl, and Li_2O, in addition to H_2O, on the melting temperatures of albite and granite. American Journal of Science, 262, 930–939.

Yoder, H.S. (1950) High-low quartz inversion up to 10,000 bars. American Geophysical Union Transactions, 31, 827–835.